

Biomarkers Associated with CD8+ T Cell Infiltration in Childhood AML

Jiafeng Zheng

Tianjin Children's Hospital (Tianjin University Children's Hospital)

Caili Zhou

Tianjin Children's Hospital (Tianjin University Children's Hospital)

Tongqiang Zhang

Tianjin Children's Hospital (Tianjin University Children's Hospital)

Wei Guo

Tianjin Children's Hospital (Tianjin University Children's Hospital)

Xiaojian Cui

Tianjin Children's Hospital (Tianjin University Children's Hospital)

Chunjiao Han

Tianjin Medical University

Yongsheng Xu

Tianjin Children's Hospital (Tianjin University Children's Hospital)

Chunquan Cai (✉ cqcns6@126.com)

Tianjin Children's Hospital (Tianjin University Children's Hospital)

Research Article

Keywords: CD8+ T cell, prognostic biomarkers, acute myelogenous leukemia, children, immune infiltration

Posted Date: July 6th, 2021

DOI: <https://doi.org/10.21203/rs.3.rs-659529/v1>

License:  This work is licensed under a Creative Commons Attribution 4.0 International License.

[Read Full License](#)

Biomarkers associated with CD8+ T cell infiltration in childhood AML

Jiafeng Zheng^{1#}, Caili Zhou^{2#}, Tongqiang Zhang^{1#}, Wei Guo¹, Xiaojian Cui³, Chunjiao Han⁴, Yongsheng Xu^{1*}, Chunquan Cai^{5*}

¹Department of pediatric respiratory medicine, Tianjin Children's Hospital (Tianjin University Children's Hospital), Tianjin, China

²Department of science and education, Tianjin Children's Hospital (Tianjin University Children's Hospital), Tianjin, China

³Department of Clinical Lab, Tianjin Children's Hospital (Tianjin University Children's Hospital), Tianjin, China

⁴Department of Children's Clinical College, Tianjin Medical University, Tianjin, China

⁵Tianjin Institute of Pediatrics (Tianjin Key Laboratory of Birth Defects for Prevention and Treatment), Tianjin Children's Hospital (Tianjin University Children's Hospital), Tianjin, China, Tianjin, China

#These authors contributed equally to this work.

*Correspondence author.

Yongsheng Xu: Department of pediatric respiratory medicine, Tianjin Children's Hospital (Tianjin University Children's Hospital), Tianjin, China. Email: xxyyss@126.com;

Chunquan Cai: Tianjin Institute of Pediatrics (Tianjin Key Laboratory of Birth Defects for Prevention and Treatment), Tianjin Children's Hospital (Tianjin University Children's Hospital), Tianjin, China. Email: cqcns6@126.com.

Abstract

Acute myeloid leukemia (AML) is a common hematological malignant tumor in children. AML is characterized by high morbidity, recurrence and mortality rates worldwide. Immune cell infiltration in tumor microenvironment plays an important role in tumor progression. This study aimed at exploring biomarkers related to CD8+ T cell infiltration in children with AML. Transcriptome data and clinical data were retrieved from TARGET database. We collected whole blood samples from some AML children to verify the results. Through the joint analysis of the data of multiple databases we found that CAMK2D, MPZL3, MSL3 are associated with CD8+ immune infiltration. Through PCR analysis, it was found that CAMK2D, MPZL3, MSL3 was highly expressed in the whole blood of children with AML. Analysis showed that CAMK2D, MPZL3 and MSL3 are potential clinical prognostic markers related to CD8+ T cell infiltration in children with AML. The findings of this study show that CAMK2D, MPZL3, MSL3 are implicated in prognosis of AML. Notably, the three genes are implicated in CD8+ T cells-related pathways.

Keywords: CD8+ T cell; prognostic biomarkers; acute myelogenous leukemia; children; immune infiltration

Introduction

Leukemia is the most common hematological malignancies in children, with a mortality rate of 4% worldwide¹. Leukemia can be grouped into lymphocytic leukemia and myelogenous leukemia based on the source of hematopoietic primordial cells. Childhood leukemia has the highest recurrence rate of acute myeloid leukemia in the world. It is responsible for the highest number of leukemia-related deaths. Childhood leukemia is characterized by multiple organ metastasis and poor prognosis. Currently, diagnosis of leukemia is mainly carried out through bone marrow biopsy. However, carrying out bone marrow biopsy in children is challenging. In addition, multiple bone marrow aspiration examinations are needed for accurate diagnosis, which further weakens the body and affects psychology of the child. Although several studies have explored

pathogenesis of AML, AML remains a health burden due to high morbidity and mortality rates. Advances in bioinformatics have enabled deposition of large gene chip sequencing data sets and clinical data of AML patients in tumor public database. Multi-directional analysis of chip data and clinical data of AML patients will help in identifying effective markers for diagnosis and prognosis of AML. These findings will provide a basis for more accurate clinical diagnosis and treatment of AML.

Previous studies show that tumor microenvironment (TME) plays an important role in tumor development. Cancer cells and surrounding Sertoli cells promote malignant phenotypes of cancer, such as malignant proliferation, resistance to apoptosis and evasion of immune surveillance. Therefore, TME plays a key role in prognosis and progression of different cancer types. TME is mainly composed of stromal cells and immune cells. Previous studies report that stromal cells are implicated in tumor angiogenesis and extracellular matrix remodeling. However, the role of immune cells found in TME on tumor growth and development have not been fully explored. Studies report that tumor infiltrating immune cell (TIC) in TME is a potential biomarker for therapeutic efficacy^{2,3}.

Infiltration of CD8+T cells in tumors and phagocytosis of related macrophages determines effectiveness of cancer immunotherapy. A recent study found that leukemia inhibitory factor (LIF), a secreted cytokine regulates CD8+T cell tumor invasion and promotes activation of tumor-associated macrophages. Inhibition of LIF reverses epigenetic silencing of CXCL9 and triggers invasion of CD8+T cell in tumors. Combination of LIF neutralization antibody and inhibition of PD1 immune checkpoint promotes elimination of tumor cells and improves survival rate of tumor patients⁴. Previous studies report that gastric cancer cells deprive CD8+T cells of glucose thus inhibiting activity of CD8+T cells. Gastric cancer cells inhibit CD8+T cell metabolism through CD155/TIGIT signaling pathway. Therefore, tumor monitoring and clearance function of CD8+T cells is affected⁵. Notably, cancer cells inhibits the function of CD8+T cells. Previous studies have shown that CD8+T cell infiltration play a key role in development of renal clear cell carcinoma. High expression levels of CCL5 gene inhibits proliferation and invasion of renal clear cell carcinoma cells. CCL5 is implicated in CD8+T cell infiltration thus it is a potential biomarker and therapeutic target of renal clear cell carcinoma⁶. Previous studies report patients with AML present with fatigue and aging of immune cells. Cancer cells directly affect activity, expansion, co-signaling and expression of CD8+T cells. Chemotherapy partly restores the function of CD8+T⁷. Role of AML in shaping response of CD8+T cells and restoration of CD8+T cell function after treatment provides a theoretical basis for new immunotherapy approach for AML. However, currently no specific molecular markers have been reported for immunotherapy against AML. Therefore, there is need to explore molecular markers related to CD8+T cellular immunity for development of AML immunotherapy.

In this study, we analyzed RNA-seq transcriptome data and clinical data of AML children. Analysis shows key regulatory genes and regulatory pathways related to CD8+ immune cells. The findings from the study provide a novel immunotherapy approach for diagnosis and treatment of AML.

Methods

1.Data collection and processing

Transcriptomic files and clinical information on childhood acute myeloid leukemia were obtained from the TARGET public database. Count data were converted into the FPKM format for subsequent verification. In this study, we constructed a weighted gene co-expression network to determine the gene module of co-expression, the relationship between gene network and phenotype, as well as the core genes in the network. The co-expression network of all genes in the dataset was constructed using WGCNA-R package. Genes with a 10000 variance were screened by this algorithm for further analysis in which the soft threshold was set at 9. The weighted adjacency matrix was transformed into the topological overlap matrix (TOM) to estimate network connectivity, while the hierarchical clustering method was used to construct the clustering tree

structure of the TOM matrix. Different branches of the cluster tree represent different gene modules while different colors represent different modules. Based on the weighted gene correlation coefficient, genes were classified according to their expression patterns. Genes with similar patterns were classified into one module.

2. Functional enrichment analysis of gene module

To determine the biological functions and signal pathways involved in the WGCNA interesting module (darkolivegreen module in this study, which has the highest correlation with phenotype), the Metascape database (www.metascape.org) was used to annotate and visualize the genes in a specific module for Gene Ontology (GO) analysis and Kyoto Encyclopedia of Gene Genome (kegg) pathway analysis. $\text{Minoverlap} \geq 3$ $p \leq 0.01$ was considered to be statistically significant.

3. Immune gene correlation

Gene effects on immune infiltration was evaluated. CIBERSORT was used to quantify the level of immune cell infiltration in each sample, and the correlation between gene expression and immune cell content was analyzed by spearman rank correlation.

4. TCGA data acquisition

The TCGA database (<https://portal.gdc.cancer.gov/>) is the largest cancer gene information database. It stores gene data, including gene expression data, miRNA expression data, copy number variation, DNA methylation, SNP and so on. We downloaded the original mRNA expression data of AML (level3 FPKM format) obtained from a total of 151 samples.

5. Gene set enrichment analysis

GSEA (gene set enrichment analysis) analysis utilizes predefined gene sets to rank genes according to their degree of differential expression between two sample types. This analysis then determines whether the predefined gene sets are enriched at the top or bottom of the ranking table. In this study, we used GSEA to compare the differences in signaling pathways between the high-risk and the low-risk groups. The comparison was done to explore the possible molecular mechanisms of the differences in prognosis between the two groups. The number of replacement was set to 1000 while the type of replacement was set to the phenotype.

6. GeneMANIA analysis

Genemania (<http://www.genemania.org>) is a flexible and user-friendly PPI network construction database. It is used to visualize functional networks between genes and to analyze gene functions as well as interactions. The website can be used to set up data sources of gene nodes, and has a variety of bioinformatics analysis methods, such as physical interaction, gene co-expression, gene co-location, gene enrichment analysis and website prediction. In this study, Genemania was used to generate the core gene network for exploring the potential mechanisms of core genes.

7. Drug sensitivity analysis

Based on the largest pharmacogenomics database (GDSC Cancer Drug sensitivity Genomics Database, <https://www.cancerrxgene.org/>), the R software package "pRRophetic" was used to predict the chemosensitivity of each tumor sample. The IC50 estimation of each specific chemotherapeutic drug treatment was obtained by regression analysis. Ten cross-validation tests were performed using the GDSC training set to verify the regression and prediction accuracy. Default values were selected for all parameters, including the "combat" function that removes the batch effect, and the average of repetitive gene expression.

8. Verification of gene expression

We collected the whole blood samples of 30 children with AML and 30 normal children as control. Through PCR quantitative analysis, we found that the expression of CAMK2D,MPZL3,MSL3 in whole blood cells of AML children was higher than that of normal children, and the difference was statistically significant.

9. Statistical analysis

All statistical analyses were performed in R language (version3.6). $p \leq 0.05$ was considered to be statistically significant.

RESULTS

1 Data collection and WGCNA analysis

The soft threshold β was determined by the function "softPowerEstimate", and was set to 9 (Figure 1A). Based on the tom matrix detection gene module, a total of 20 gene modules (Figure 1B and Figure 1C) were detected, constructed, and marked with different colors as: black, 577; blue, 1086; brown, 439; darkgrey, 150; darkmagenta, 75; darkolivegreen, 85; darkturquoise, 151; greenyellow, 588; grey, 1376; lightcyan, 226; lightgreen, 197; lightyellow, 193; orange, 149; paleturquoise, 2073; pink, 1016; and purple, 973. We found that the darkolivegreen module had the highest immunophenotypic correlation with CD8+ T cells ($cor=0.55$, $p=2e-28$). Therefore, the darkolivegreen module was selected for follow-up verification. The constituent genes in the darkolivegreen module were selected and their correlation with CD8+ immune cell characteristics determined(Figure 1D). A significant correlation was found ($cor=0.71$, $p=2.8e-14$).

2. GO and KEGG analysis.

The darkolivegreen module genes were selected for GO and KEGG analysis(Figure 2A). It was revealed that the darkolivegreen module mainly enriched T cell activation(Figure 2B), T cell receptor signaling pathway, Antigen receptor-mediated signaling pathway, Alpha-beta T cell activation and other signal mechanisms that are associated with T cells. It is speculated that the influence of darkolivegreen module on AML progression is closely related to the above pathway. The interactions between the modules are as shown in the PPI diagram(Figure 2C).

3. KM-plot survival analysis

By selecting the darkolivegreen module genes and performing KM-plot survival analysis(Figure 3), we established the relationship between these genes and the prognosis of AML patients. The core genes associated with AML progression were screened out. A total of 10 genes (ZAP70, BIRC3, CAMK2D, CD6, ERP27, LY9, MPZL3, MSL3, OXNAD1 and TMEM2) are closely associated with AML prognosis. Exploring the potential mechanism of these genes in AML and describing the molecular map of immune-related therapy for AML will be helpful in the therapeutic management of AML.

4. Internal and external interactions of core genes

Tumor microenvironment is mainly composed of tumor-associated fibroblasts, immune cells, extracellular matrix, a variety of growth factors, inflammatory factors, special physical and chemical characteristics and cancer cells. The tumor microenvironment significantly affects tumor diagnosis, survival outcomes and sensitivity to clinical therapy. We found that the 10 genes were closely correlated with immune cell infiltration, while 9 genes(ZAP70, BIRC3, CAMK2D, CD6, ERP27, LY9, MPZL3, OXNAD1 and TMEM2) were associated with CD8+ cells of AML(Figure 4A), which further validates our previous results. In addition, we downloaded the first 20 genes that are highly associated with AML in children from the Genecards database. We analyzed their correlation with the expression of core genes. The results showed that the 10 core genes were closely correlated with the first 20 AML-associated genes(Figure 4B). The Circos diagram shows the interaction of these 10 genes(Figure 4C). The Genemania diagram shows that the 10 genes are involved in the adjacent network(Figure 4D), which implies that the core genes are involved in immune mechanisms such

as lymphocyte activation, T cell activation and leukocyte activation.

5. TCGA database verification

To verify the roles of the 10 genes in AML, we extracted transcriptomic and clinical data from the TCGA database. The findings of the KM-plot suggested that CAMK2D ($p=1.021e-03$), MPZL3 ($p=8.941e-04$) and MSL3 ($p=3.897e-02$) could predict the prognosis of AML patients (Figure 5A). The immune infiltration analysis of TCGA-AML expression profile showed that MSL3 and MPZL3 were closely correlated with CD8+ (Figure 5B). We further determined the sensitivity of core genes to common chemotherapeutic drugs. Based on the drug sensitivity data obtained from the GDSC database, we used R packet "pRRophetic" to predict the chemosensitivity of each tumor sample. The results revealed that the high and low expression levels of CAMK2D, MPZL3 and MSL3 affected the sensitivity to common chemotherapeutic drugs (Docetaxel and Paclitaxel) (Figure 6A, Figure 6B and Figure 6C).

6. MSI and GSEA analysis

Microsatellite instability (MSI) refers to the increase or loss of simple repetitive sequences in the genome. MSI is prevalent in many tumors. Because of the significant correlation between MSI and immune checkpoint blocking response, MSI can be used to predict tumor responses to immunotherapy. In this study, analysis of the relationship between core genes and MSI revealed that a high expression of MPZL3 was associated with increased MSI instability (paired 0.031). We then determined the specific signaling pathways involved in the three cores and explored the potential molecular mechanisms by which core genes affect AML progression. GSEA results showed that: overexpressed CAMK2D genes were involved in the B cell receptor signaling pathway (Figure 7A), Pantothenate and CoA biosynthesis as well as in Th1 and Th2 cell differentiation signaling pathways (Figure 8A and Figure 8B); overexpressed MPZL3 genes (Figure 7B) were involved in antigen processing and presentation, galactose metabolism and Th17 cell differentiation signaling pathways (Figure 8C and Figure 8D) while overexpressed MSL3 genes (Figure 7C) were involved in Toll-like receptor signaling pathway (Figure 8E and Figure 8F), Autoimmune thyroid disease and Th17 cell differentiation signaling pathways.

7. Experimental verification

The whole blood samples of 30 AML children and 30 healthy children were collected and compared. The expression of three genes was analyzed by PCR. It was found that CAMK2D, MPZL3, MSL3 was highly expressed in the whole blood cells of AML children (Figure 9A, Figure 9B and Figure 9C). The statistical analysis showed that the difference was statistically significant.

Discussion

AML is the most common non-solid tumor in children worldwide. AML is characterized by high prevalence and mortality rate of AML, therefore it is a major burden in children¹. Accurate diagnosis of AML is achieved through bone marrow biopsy. Diagnostic accuracy of bone marrow puncture varies with clinical stage of AML, therefore, multiple biopsies may be required for accurate diagnosis. These several biopsy procedures delay diagnosis and treatment of AML. In some cases, recurrent refractory AML is not sensitive to chemotherapeutic drugs, thus affecting survival rate of AML patients. Currently, chemotherapy is the main treatment approach for AML. Late diagnosis of AML results in high degree of malignancy and lack of sensitivity to chemotherapeutic drugs at the time of diagnosis. Although, several studies have explored diagnosis and treatment approaches for AML, it remains a major health burden in children due to high

mortality and recurrence rate of AML. Advances in gene technology in recent years, have resulted in availability of transcriptome and immune cell data for blood and bone marrow samples of children. Large amounts of AML gene chip data and clinical data are available in public databases. Previous studies have explored immunotherapy targets related to tumor immune cell activity through analysis of chip data of cancer patients. Recent studies report that the abnormal function of immune cells play an important role in of cancer prognosis and restoration of function of immune cells prevent cancer progression⁸. In addition, studies report that high expression levels of TIGIT on the surface of CD8+ cells in patients with AML inhibits antitumor activity of T cells, and is positively correlated with poor clinical prognosis of AML. Blocking expression of TIGIT to restore T cell function and anti-tumor activity can be a novel and effective treatment for leukemia⁹. Therefore, components and function of immune cells in tumor microenvironment play a key role diagnosis, treatment and prognosis of different cancer tumors. In this study, explored diagnostic, therapeutic and prognostic targets against AML in children through analysis of AML chip data and clinical data. to the findings of this study can be used for timely AML diagnosis, for development of novel chemotherapeutic drugs, and for AML prognosis.

We constructed WGCNA network using transcriptome data and clinical data of target database. Analysis showed that biomarkers involved in immune infiltration in children with AML found have immunophenotypic correlation with T cells CD8+. GO and KEGG analysis showed that signaling pathway related to T cells is highly enriched. Survival analysis showed that ZAP70, BIRC3, CAMK2D, CD6,ERP27, LY9,MPZL3, MSL3, OXNAD1 and TMEM2 genes are associated with AML prognosis. Further, these genes were implicated in pathways related to T cells and other immune cell functions. Analysis of AML related data in TCGA database showed that CAMK2D, MPZL3 and MSL3 are correlated with AML prognosis. Furthermore, expression levels of CAMK2D, MPZL3 and MSL3 are related to activity of Docetaxel and Paclitaxel which are common chemotherapeutic drugs. These two drugs are not commonly used in treatment of AML children, however, previous studies report that paclitaxel combined with metformin is effective in treatment of AML subtypes¹⁰. Currently, no studies have reported direct use of Paclitaxel for AML treatment. MSI and GSEA pathway analysis showed that high expression levels of MPZL3 are correlated with increased instability of MSI. In addition, high expression levels of MPZL3 were correlated with signaling pathway of immune cells.

Recent studies reported presence of CD8+ immune cells in 6 different malignant tumors. Therefore, an immunotherapy based on CD8+ can be used for cancer treatment. Identification of tumor antigen-specific T cells from cancer patients is key in development of immunotherapy, diagnosis and treatment approaches¹¹. In addition, a previous study explored anti-tumor activity of dendritic cells by cross-activating CD8 cells and presenting foreign antigens to activate CD8+T cells¹². Fibroblasts in tumor microenvironment affect activity and function of CD8+ in tumor through IL6¹³. Furthermore, fibroblast play a role in killing and scavenging function of CD8+ cells in tumors. A previous study on tumor immune microenvironment in 203small cell lung cancer showed that low levels of CD8+ immune cells is positively correlated with poor prognosis of small cell lung cancer¹⁴. CD8+ cells are tumor-specific immune cells generally present in tumor microenvironment of cancer patients, however, their levels and activity are affected by several factors.

CD8+T cell immune surveillance plays an important role in solid tumors and T cell dysfunction promotes tumor progression. Gene expression pattern of CD8+T cells is related with AML prognosis. Further, activity of CD8+T cells is regulated by different genes and molecular pathways¹⁵. A prospective randomized controlled trial of 79 AML patients showed immunodeficiency of T cells and natural killer (NK) cells. During diagnosis, CD8+T cells and CD4+T cells were aged and had no activity¹⁶. Quantitative analysis of T cell infiltration in bone marrow biopsies of patients with AML showed a higher percentage of CD8+ positive T cells in bone marrow of patients with multiple relapse compared with the levels of patients with first

recurrence or newly diagnosed AML¹⁷. A previous study reports that mP3-expressing PMN significantly inhibits autologous healthy donor T cell proliferation. However, mP3-expressing PMN does not affect cytokine production in activated T cells. Activity of mP3-expressing PMN on T cells requires cell proximity and is abrogated by P3 inhibition¹⁸.

In this study, we report that CD8+ cells are significantly correlated with prognosis of AML. Moreover, CAMK2D, MPZL3, MSL3 were implicated in regulatory pathway of T cells which is correlated with function and activity of CD8+ cells, thus can be used in AML prognosis.

CAMK2D is an interferon- γ -induced gene. Interferon- γ promotes expression of PD-L1 in tumor microenvironment. Expression level of tumor infiltrating T cells is positively correlated with expression of PD-L1 in mouse in situ glioma model and human glioma. These findings imply that CAMK2D is involved in distribution of tumor infiltrating T cells by regulating expression of PD-L1¹⁹. In addition, overexpression of CAMK2D affects multiple metabolic and cancer-related signaling pathways involved in response to cisplatin therapy and development of drug resistance. Therefore, expression of CAMK2D gene modulates distribution and content of tumor infiltrating T cells, affects drug resistance in tumors, and indirectly affects treatment and prognosis of tumor²⁰.

MPZL3 protein resides in the mitochondria. MPZL3 is protein coding gene implicated in seborrheic dermatitis²¹. Studies have shown that expression of MPZL3 is associated with different cancer types. A previous study reports that MPZL3 is associated with lung cancer susceptibility²². A study on microarray analysis showed that MPZL3 is highly expressed in rectal cancer cells²³. These findings imply that MPZL3 is a cancer-related gene.

MSL3 plays an important role in human development in the human body, and its mutation results in systemic growth retardation, progressive gait disorders and recognizable facial deformities²⁴. Low expression levels of MSL3 are associated with ovarian cancer. MSL3 inhibits malignant phenotype of ovarian cancer cells. In addition, low expression levels of MSL3 is associated with poor prognosis of ovarian cancer²⁵. Therefore, low expression levels of MSL3 are associated with occurrence and development of malignant tumors, which indirectly affects prognosis and survival outcome of patients with tumors.

In this study, through the joint analysis of three databases, three genes with diagnostic value for AML were found. Through the pathway and enrichment analysis of genes, it was found that these three genes were associated with CD8+ cells. As a common hematological tumor in children, through the collection of clinical blood samples for nearly a year, through the quantitative PCR analysis of CAMK2D,MPZL3,MSL3, it was found that there was a clear high expression in the whole blood cells of AML children. As a kind of hematological tumor with high mortality, AML has systemic distribution, no designated target organs, and high mortality, so it is difficult to carry out further clinical trials to verify the deep pathway and function of a certain gene, while animal experiments are difficult to completely simulate the environment of human bone marrow for the production of cancer blood cells, so the verification is limited to the study of gene expression. It is still necessary for more scholars to conduct more in-depth basic research on the specific and detailed regulatory mechanism of these three genes on CD8+ cells in AML, so as to provide a new idea for immunotherapy for children with AML.

In summary, we conducted a multi-angle analysis of transcriptome data and clinical data of AML patients. The findings of the study show that CD8+ cells in tumor microenvironment is correlated with prognosis of AML. Further studies should be carried out to explore the role of CAMK2D, MPZL3, MSL3 genes in regulation of CD8+ cell activity and their clinical significance.

- Myeloid Leukemia. LID - 10.3390/cancers12061634 [doi] LID - 1634. (2020).
- 2 Wood, S. L., Pernemalm, M., Crosbie, P. A. & Whetton, A. D. The role of the tumor-microenvironment in lung cancer-metastasis and its relationship to potential therapeutic targets. doi:10.1016/j.ctrv.2013.10.001.
- 3 Quail, D. F. & Joyce, J. A. Microenvironmental regulation of tumor progression and metastasis. doi:10.1038/nm.3394.
- 4 Pascual-García, M. A.-O. *et al.* LIF regulates CXCL9 in tumor-associated macrophages and prevents CD8(+) T cell tumor-infiltration impairing anti-PD1 therapy. (2019).
- 5 He, W. *et al.* CD155T/TIGIT Signaling Regulates CD8(+) T-cell Metabolism and Promotes Tumor Progression in Human Gastric Cancer. (2017).
- 6 Lin, J. *et al.* Identification of biomarkers related to CD8(+) T cell infiltration with gene co-expression network in clear cell renal cell carcinoma. (2020).
- 7 Knaus, H. A. *et al.* Signatures of CD8+ T cell dysfunction in AML patients and their reversibility with response to chemotherapy. (2018).
- 8 Smith, T. T. *et al.* In situ programming of leukaemia-specific T cells using synthetic DNA nanocarriers. (2017).
- 9 Kong, Y. *et al.* T-Cell Immunoglobulin and ITIM Domain (TIGIT) Associates with CD8+ T-Cell Exhaustion and Poor Clinical Outcome in AML Patients. (2016).
- 10 Asik, A. *et al.* Antileukemic effect of paclitaxel in combination with metformin in HL-60 cell line. (2018).
- 11 Duhén, T. *et al.* Co-expression of CD39 and CD103 identifies tumor-reactive CD8 T cells in human solid tumors. (2018).
- 12 Fu, C. & Jiang, A. Dendritic Cells and CD8 T Cell Immunity in Tumor Microenvironment. (2018).
- 13 Kato, T. *et al.* Cancer-Associated Fibroblasts Affect Intratumoral CD8(+) and FoxP3(+) T Cells Via IL6 in the Tumor Microenvironment. (2018).
- 14 Kinoshita, F. *et al.* Combined Evaluation of Tumor-Infiltrating CD8 + and FoxP3 + Lymphocytes Provides Accurate Prognosis in Stage IA Lung Adenocarcinoma. (2020).
- 15 Radpour, R. A.-O. *et al.* CD8(+) T cells expand stem and progenitor cells in favorable but not adverse risk acute myeloid leukemia. (2019).
- 16 Tang, L. *et al.* Characterization of Immune Dysfunction and Identification of Prognostic Immune-Related Risk Factors in Acute Myeloid Leukemia. (2020).
- 17 Williams, P. *et al.* The distribution of T-cell subsets and the expression of immune checkpoint receptors and ligands in patients with newly diagnosed and relapsed acute myeloid leukemia. (2019).
- 18 Yang, T. H. *et al.* Membrane-Associated Proteinase 3 on Granulocytes and Acute Myeloid Leukemia Inhibits T Cell Proliferation. (2018).
- 19 Qian, J. *et al.* The IFN- γ /PD-L1 axis between T cells and tumor microenvironment: hints for glioma anti-PD-1/PD-L1 therapy. (2018).
- 20 Nguyen, T. & Shively, J. E. Induction of Lumen Formation in a Three-dimensional Model of Mammary Morphogenesis by Transcriptional Regulator ID4: ROLE OF CaMK2D IN THE EPIGENETIC REGULATION OF ID4 GENE EXPRESSION. (2016).
- 21 Wikramanayake, T. A.-O. *et al.* Increased IL-17-expressing $\gamma\delta$ T cells in seborrhoeic dermatitis-like lesions of the Mpz13 knockout mice. (2018).

- 22 Wang, Y. A.-O. *et al.* Integrating expression-related SNPs into genome-wide gene- and pathway-based analyses identified novel lung cancer susceptibility genes. (2018).
- 23 Kim, S. C., Shin, Y. K., Kim, Y. A., Jang, S. G. & Ku, J. A.-O. Identification of genes inducing resistance to ionizing radiation in human rectal cancer cell lines: re-sensitization of radio-resistant rectal cancer cells through down regulating NDRG1. (2018).
- 24 Basilicata, M. A.-O. *et al.* De novo mutations in MSL3 cause an X-linked syndrome marked by impaired histone H4 lysine 16 acetylation. (2018).
- 25 Yamanoi, K. A.-O. *et al.* Acquisition of a side population fraction augments malignant phenotype in ovarian cancer. (2019).

Figure 1 (A) Analyze the scale-free fit index of the 1-20 soft threshold power (β), Analyze the average connectivity of 1-20 soft threshold power. (B) Genes are grouped into various modules by hierarchical clustering, and different colors represent different modules. (C) Heatmap shows correlations of module eigengenes with T-cell infiltration. (D) A scatter plot of the genes in the darkolivegreen module. Each bubble represents a gene, and the correlation between module membership and gene significance.

Figure 2 (A) The first 20 enriched terms are shown as a bar chart. (B) The network diagram is constructed with each enrichment term as a node and the similarity of the node as the edge. Nodes with the same cluster ID are the same color. (C) PPI network of the hub genes from the darkolivegreen module. The higher the number of connected nodes, the larger the size of the node.

Figure 3 Kaplan-Meier analysis. The overall survival analysis of ZAP70, BIRC3, CAMK2D, CD6 ERP27, LY9, MPZL3, MSL3, OXNAD1, TMEM2.

Figure 4 (A) Heatmap shows correlations of ten hub genes with T-cell infiltration. (B) Heatmap shows correlations of ten hub genes and the top 20 genes most related to AML in children that selected from Genecards database. (C) Internal interaction between the 10 hub genes. (D) The most relevant interaction networks and functional networks between these 10 hub genes and neighboring genes.

Figure 5 (A) Download the data from the TCGA database to verify the accuracy of the 10 selected hub genes in predicting the diagnosis and prognosis of AML diseases. It was found that the expression of 3 genes (CAMK2D, MPZL3, MSL3) was significantly related to the survival time of AML children. (B) Heatmap shows correlations of 3 genes (CAMK2D, MPZL3, MSL3) with T-cell infiltration.

Figure 6 Analysis of Drug sensitivity data based on GDSC Database. (A) Sensitivity of CAMK2D expression to common chemotherapeutic drugs in children with AML. (B) Sensitivity of MPZL3 expression to common chemotherapeutic drugs in children with AML. (C) Sensitivity of MSL3 expression to common chemotherapeutic drugs in children with AML.

Figure 7 The relationship between hub genes and MSI (microsatellite instability). (A) The relationship between CAMK2D and MSI. (B) The relationship between MPZL3 and MSI. (C) The relationship between MSL3 and MSI.

Figure 8 (A) The circle diagram shows three enrichment pathways and the CAMK2D gene that play a role in the enrichment process. The larger the circle corresponding to each gene, the larger the rank metric score value. (B) The above picture shows the enrichment fractional broken line of the three pathways, and the lines in the lower figure correspond to the CAMK2D gene of each pathway. (C) The circle diagram shows three enrichment pathways of CAMK2D gene. (D) The GSEA show the specific enrichment signal pathways of MPZL3 gene. (E) The circle diagram shows three enrichment pathways of MSL3 gene. (F) The GSEA show the specific enrichment signal pathways of MSL3 gene.

Figure 9 (A) Expression of CAMK2D in whole blood samples of children with AML and normal children. (B) Expression of MPZL3 in whole blood samples of children with AML and normal children. (C) Expression of MSL3 in whole blood samples of children with AML and normal children.

Figures

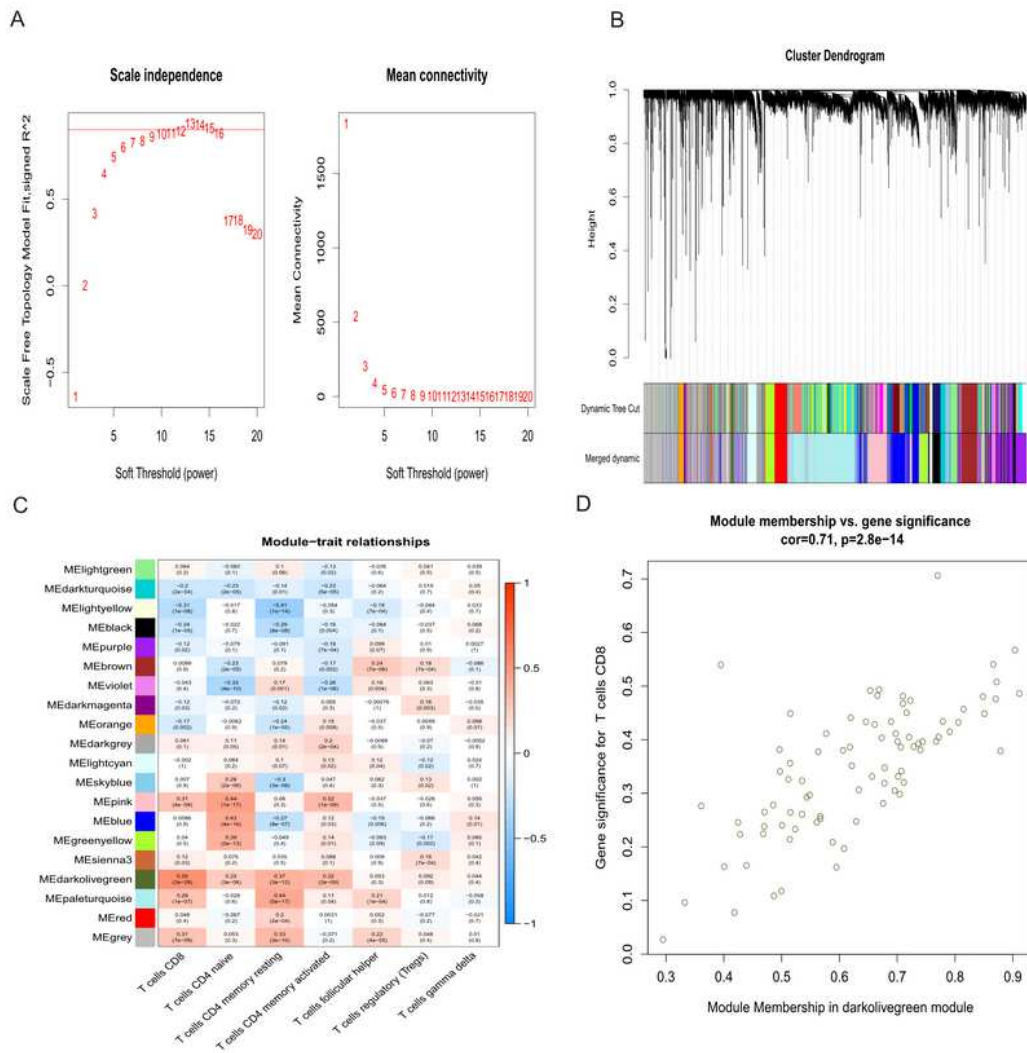
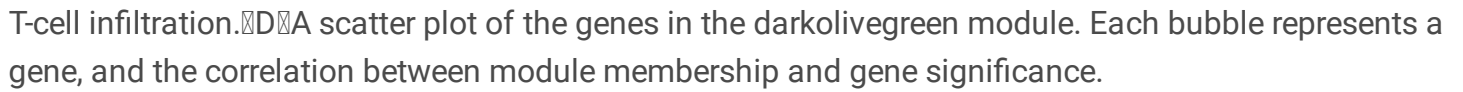


Figure 1

A Analyze the scale-free fit index of the 1-20 soft threshold power (β), Analyze the average connectivity of 1-20 soft threshold power.
 B Genes are grouped into various modules by hierarchical clustering, and different colors represent different modules.
 C Heatmap shows correlations of module eigengenes with

T-cell infiltration.  A scatter plot of the genes in the darkolivegreen module. Each bubble represents a gene, and the correlation between module membership and gene significance.

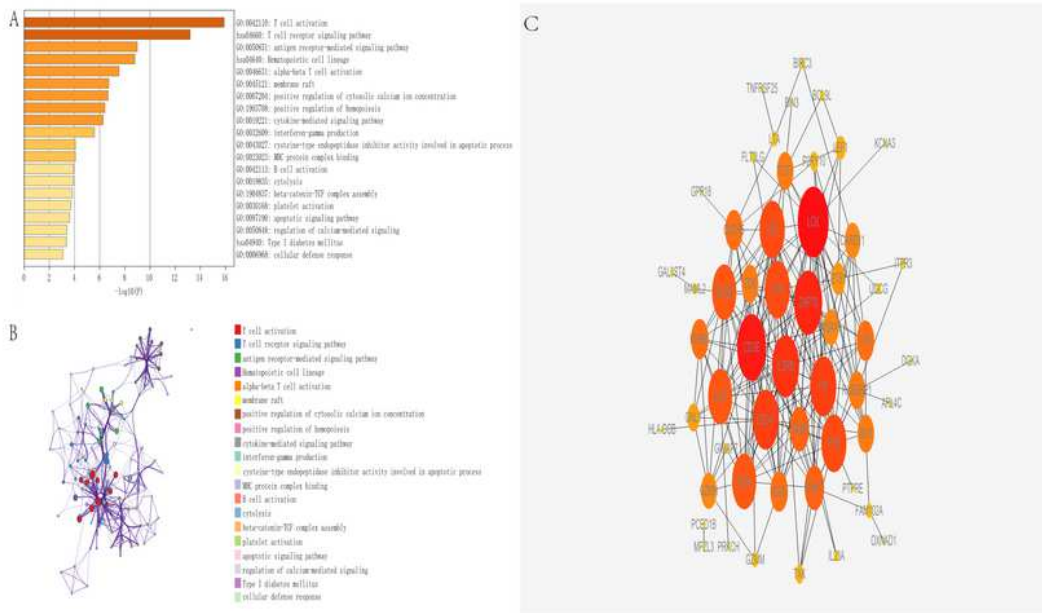


Figure 2

(A) The first 20 enriched terms are shown as a bar chart. (B) The network diagram is constructed with each enrichment term as a node and the similarity of the node as the edge. Nodes with the same cluster

ID are the same color. (C) PPI network of the hub genes from the darkolivegreen module. The higher the number of connected nodes, the larger the size of the node

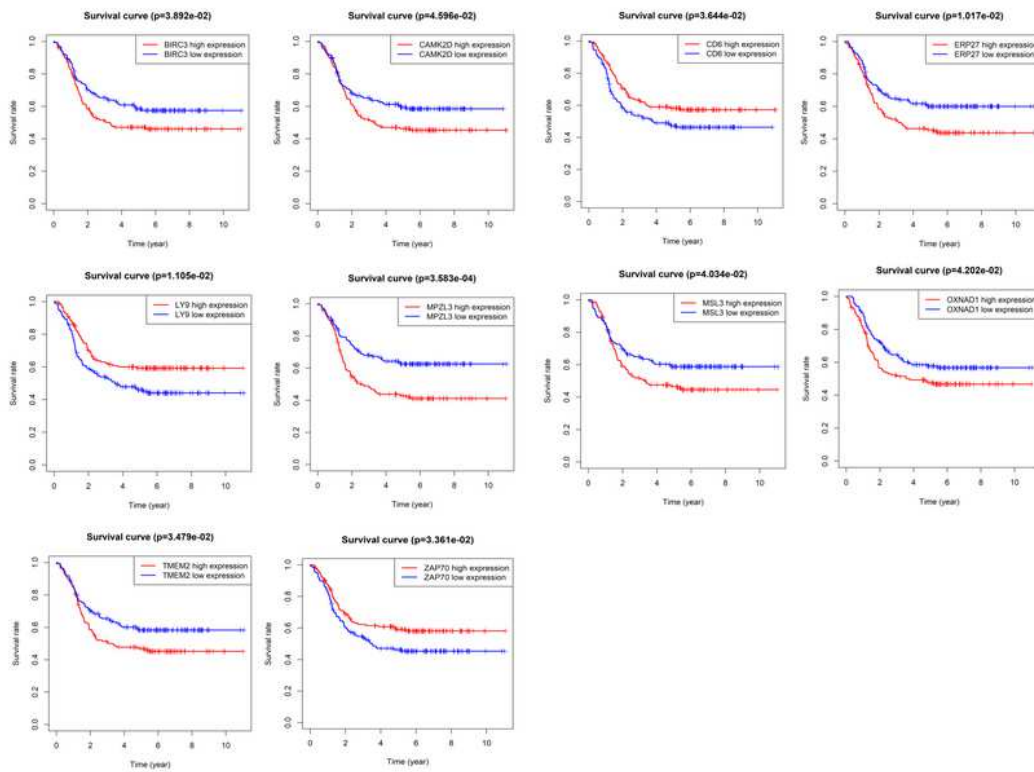


Figure 3

Kaplan-Meier analysis. The overall survival analysis of ZAP70,BIRC3,CAMK2D,CD6 ERP27,LY9,MPZL3,MSL3,OXNAD1,TMEM2.

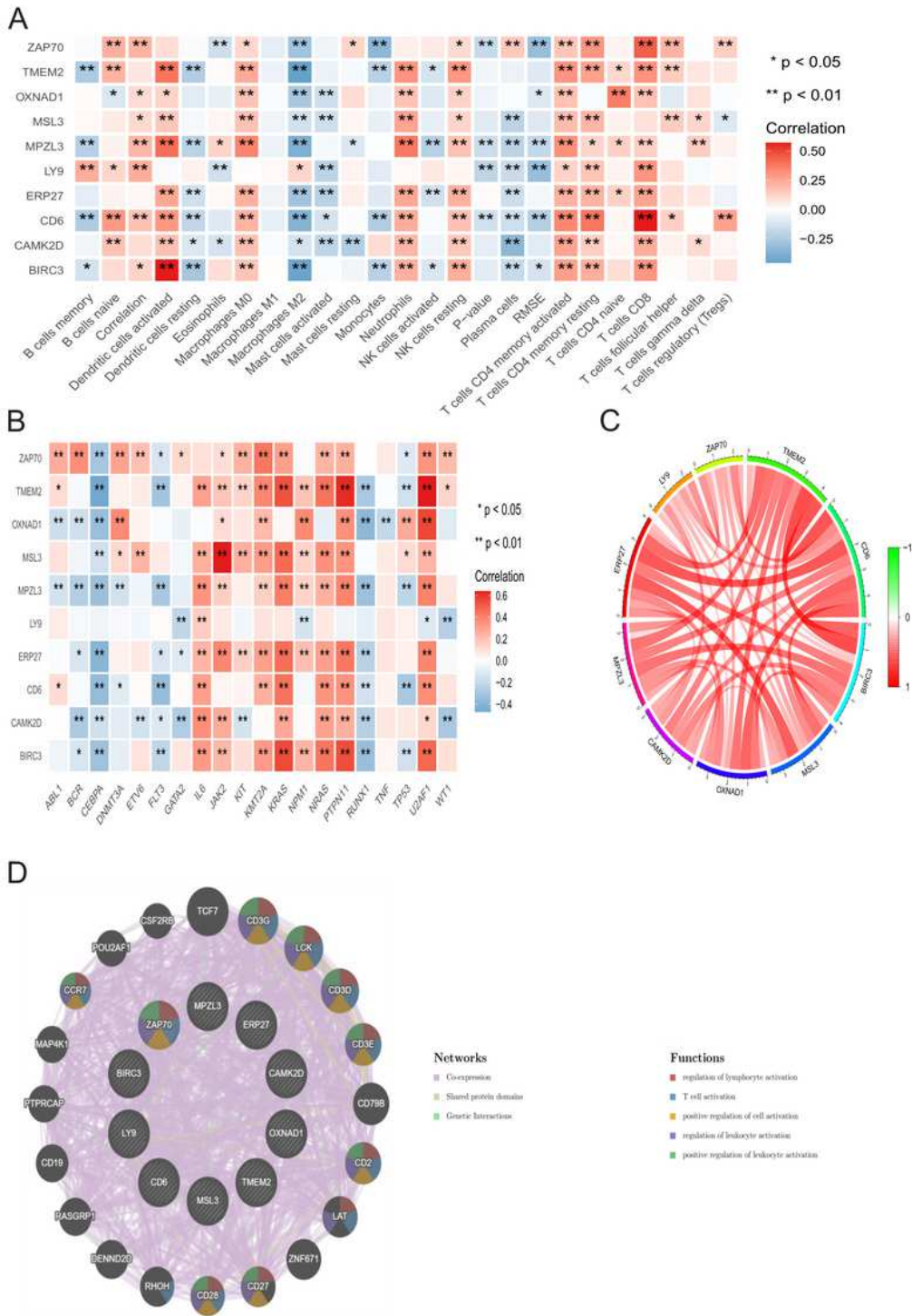


Figure 4

Heatmap shows correlations of ten hub genes with T-cell infiltration. Heatmap shows correlations of ten hub genes and the top 20 genes most related to AML in children that selected from Genecards database. (C) Internal interaction between the 10 hub genes. (D) The most relevant interaction networks and functional networks between these 10 hub genes and neighboring genes.

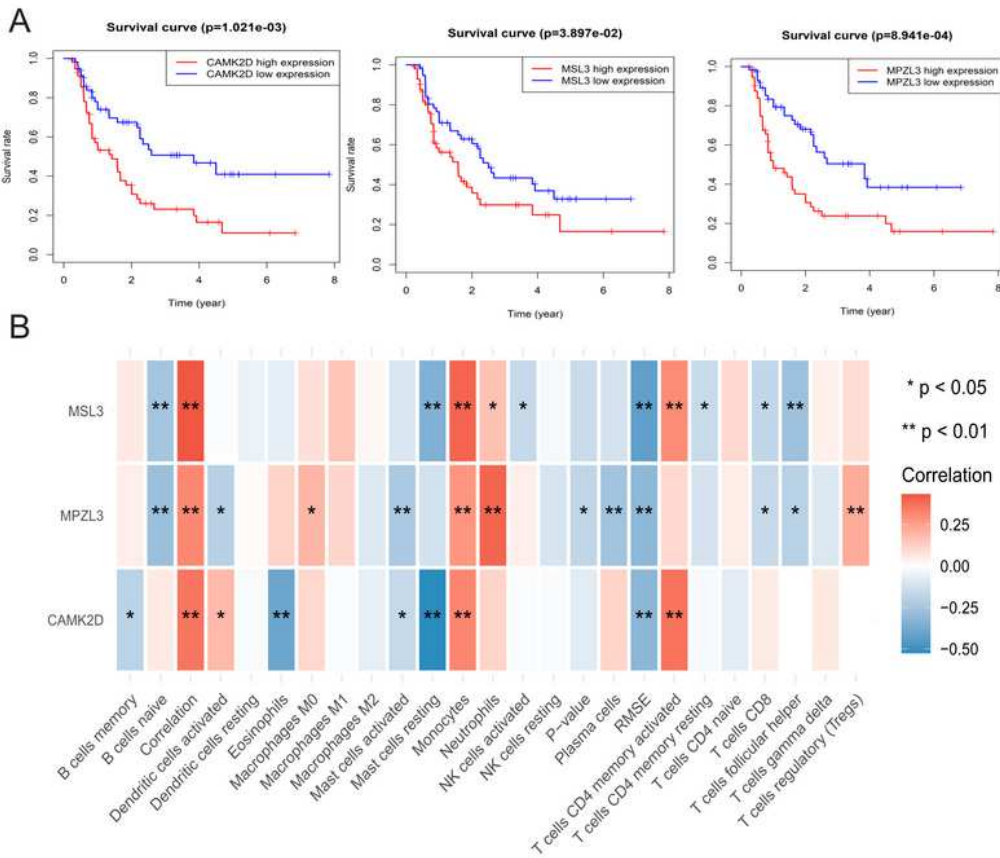


Figure 5

(A) Download the data from the TCGA database to verify the accuracy of the 10 selected hub genes in predicting the diagnosis and prognosis of AML diseases. It was found that the expression of 3 genes [CAMK2D, MPZL3, MSL3] was significantly related to the survival time of AML children. [B] Heatmap shows correlations of 3 genes (CAMK2D, MPZL3, MSL3) with T-cell infiltration.

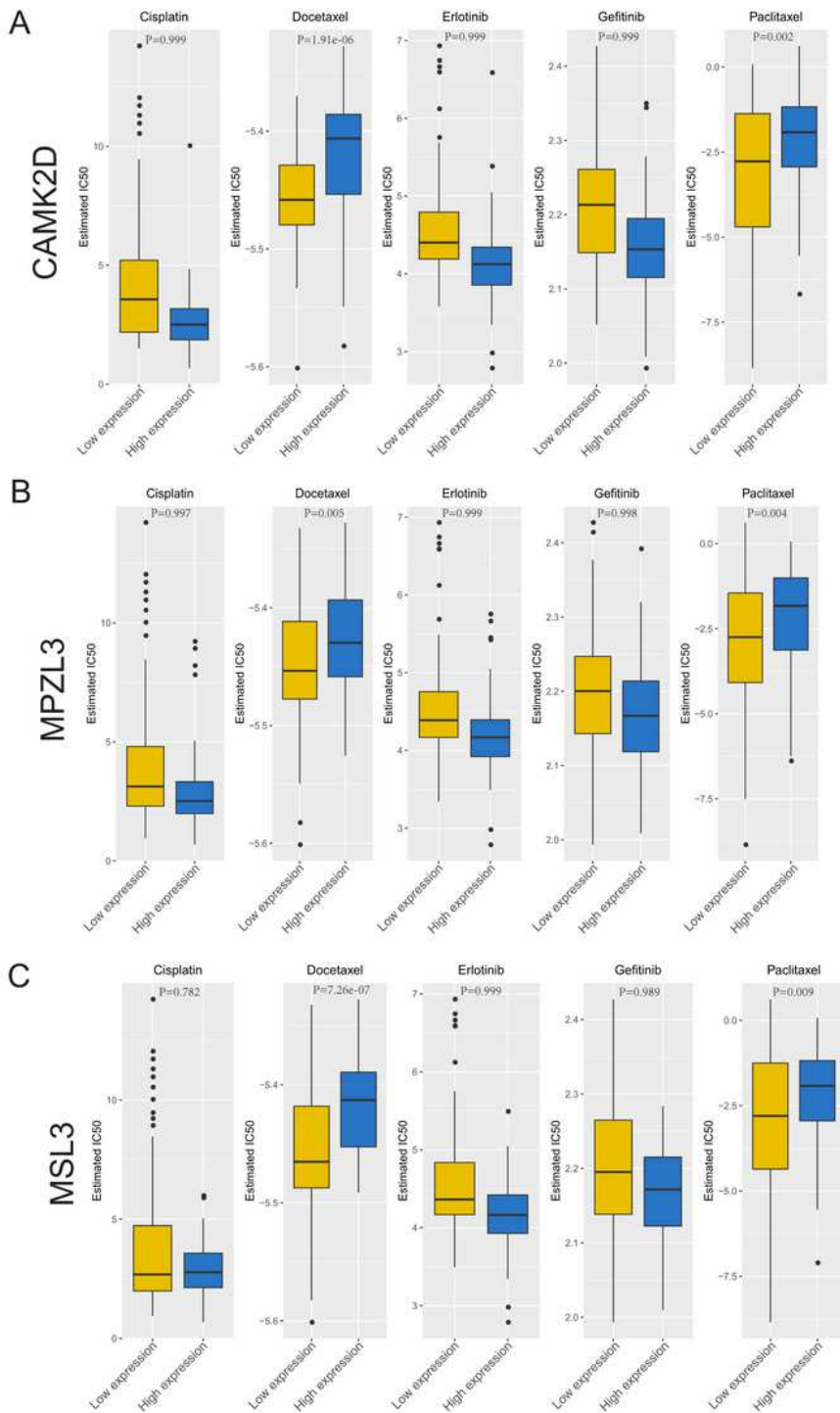


Figure 6

Analysis of Drug sensitivity data based on GDSC Database. (A) Sensitivity of CAMK2D expression to common chemotherapeutic drugs in children with AML. (B) Sensitivity of MPZL3 expression to common chemotherapeutic drugs in children with AML. (C) Sensitivity of MSL3 expression to common chemotherapeutic drugs in children with AML.

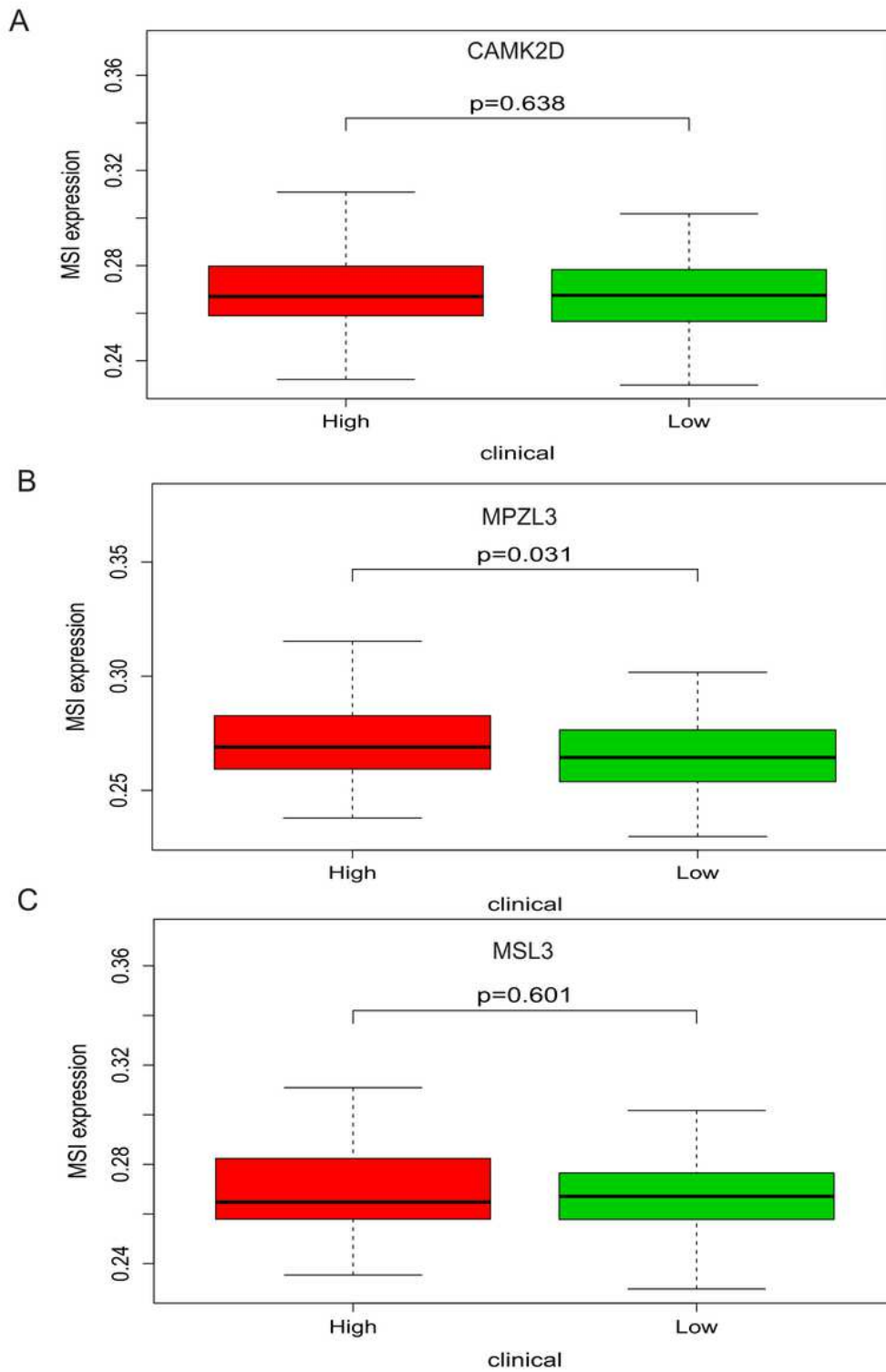


Figure 7

The relationship between hub genes and MSI(microsatellite instability). (A) The relationship between CAMK2D and MSI. (B) The relationship between MPZL3 and MSI. (C) he relationship between MSL3 and MSI

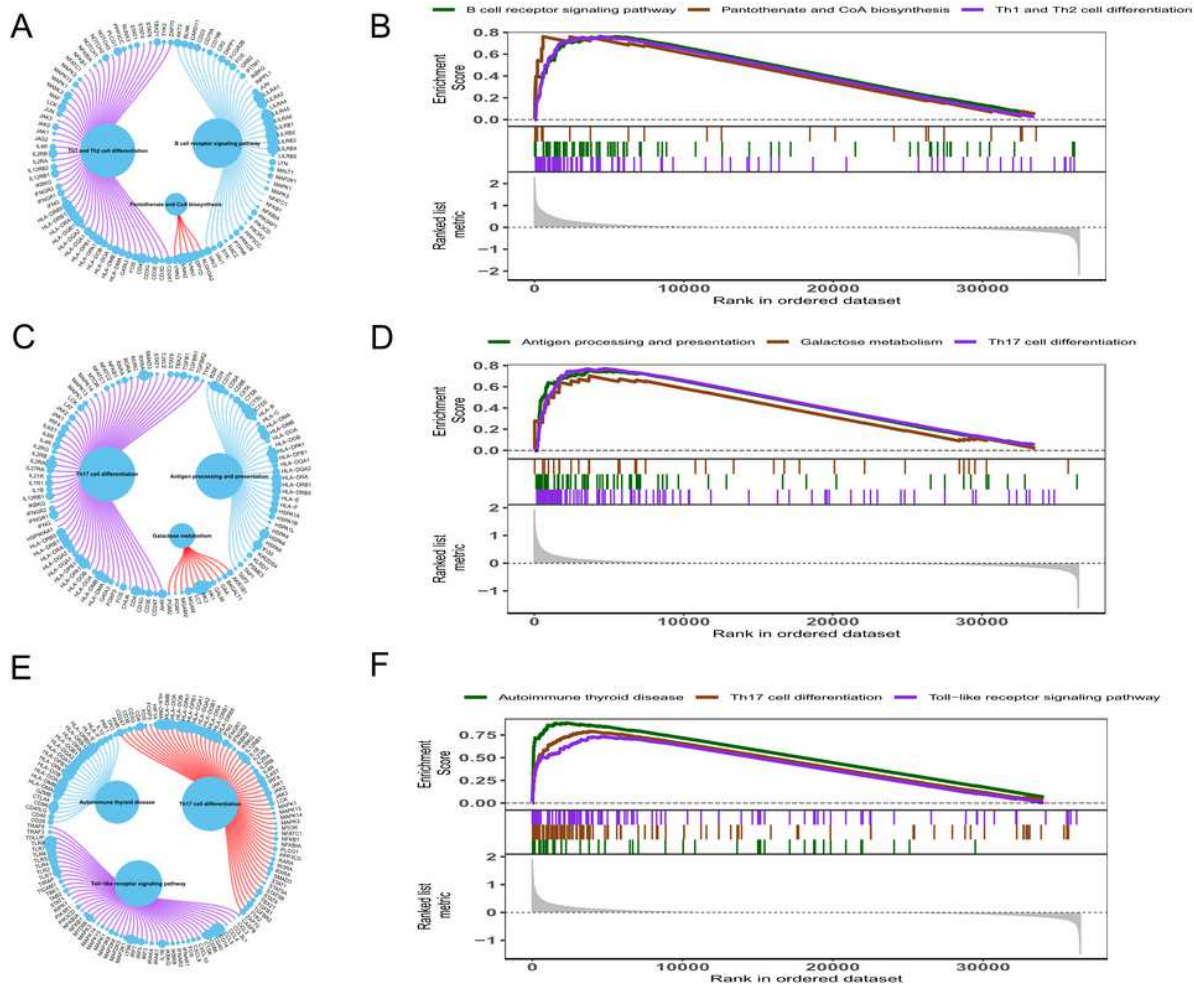


Figure 8

(A) The circle diagram shows three enrichment pathways and the CAMK2D gene that play a role in the enrichment process. The larger the circle corresponding to each gene, the larger the rank metric score value. (B) The above picture shows the enrichment fractional broken line of the three pathways, and the lines in the lower figure correspond to the CAMK2D gene of each pathway. (C) The circle diagram shows three enrichment pathways of CAMK2D gene. (D) The GSEA show the specific enrichment signal pathways of MPZL3 gene. (E) The circle diagram shows three enrichment pathways of MSL3 gene. (F) The GSEA show the specific enrichment signal pathways of MSL3 gene.

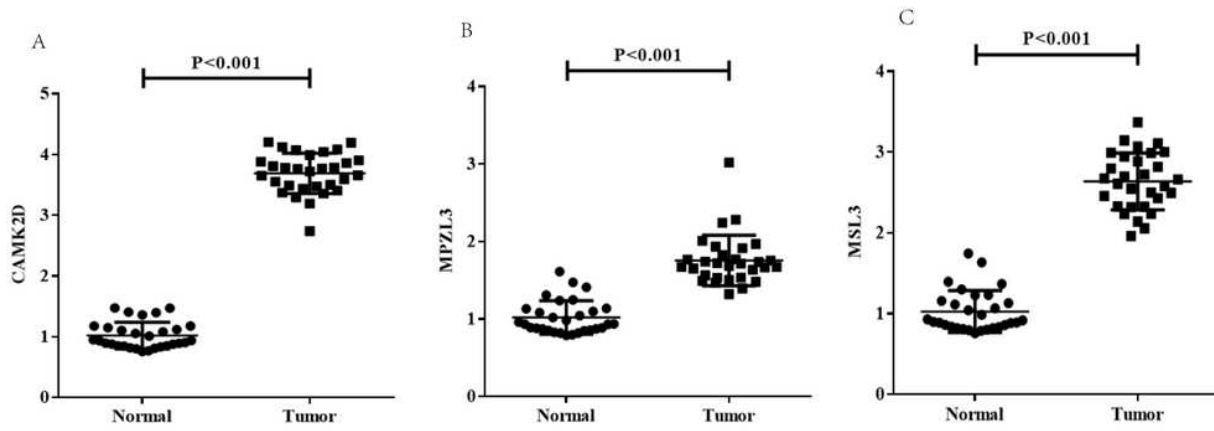


Figure 9

(A) Expression of CAMK2D in whole blood samples of children with AML and normal children. (B) Expression of MPZL3 in whole blood samples of children with AML and normal children. (C) Expression of MSL3 in whole blood samples of children with AML and normal children